Multiple ERK substrates execute single biological processes in *Caenorhabditis elegans* germ-line development

Swathi Arur[a], Mitsue Ohmachi[a], Sudhir Nayak[a,1], Matthew Hayes[a], Alejandro Miranda[a], Amanda Hay[a], Andy Golden[b], and Tim Schedl[a,2]

[a]Department of Genetics, Washington University School of Medicine, St. Louis, MO 63110; and [b]Laboratory of Biochemistry and Genetics, National Institute of Diabetes and Digestive and Kidney Diseases/National Institutes of Health, Bethesda, MD 20892-0840

Edited by Iva S. Greenwald, Columbia University, New York, NY, and approved January 23, 2009 (received for review December 5, 2008)

RAS-extracellular signal regulated kinase (ERK) signaling governs multiple aspects of cell fate specification, cellular transitions, and growth by regulating downstream substrates through phosphorylation. Understanding how perturbations to the ERK signaling pathway lead to developmental disorders and cancer hinges critically on identification of the substrates. Yet, only a limited number of substrates have been identified that function in vivo to execute ERK-regulated processes. The *Caenorhabditis elegans* germ line utilizes the well-conserved RAS–ERK signaling pathway in multiple different contexts. Here, we present an integrated functional genomic approach that identified 30 ERK substrates, each of which functions to regulate one or more of seven distinct biological processes during *C. elegans* germ-line development. Our results provide evidence for three themes that underlie the robustness and specificity of biological outcomes controlled by ERK signaling in *C. elegans* that are likely relevant to ERK signaling in other organisms: (*i*) multiple diverse ERK substrates function to control each individual biological process; (*ii*) different combinations of substrates function to control distinct biological processes; and (*iii*) regulatory feedback loops between ERK and its substrates help reinforce or attenuate ERK activation. Substrates identified here have conserved orthologs in humans, suggesting that insights from these studies will contribute to our understanding of human diseases involving deregulated ERK activity.

functional genomics | signaling | MPK-1 | RNAi screen

The RTK–RAS–ERK pathway relays extracellular signals via a conserved kinase cascade that results in phosphorylation and activation of ERK, the terminal member of this pathway (1, 2). Active ERK in turn phosphorylates substrates to execute many cellular and developmental processes (2) (Fig. 1*A*). Comprehensive insight into mechanisms underlying ERK-dependent control of biological processes depends on identification of ERK substrates. Although bona fide ERK substrates have been identified in cultured cells (3–5) and potential substrates documented from proteomic studies (6, 7), the function of most of these substrates in vivo has not been defined. Additionally, currently identified substrates do not account for most ERK-dependent events in mammals, making it likely that more substrates remain to be identified. Forward genetic studies in *Caenorhabditis elegans* and *Drosophila* have identified a few ERK substrates that act in defined biological contexts (8–10); however, the mutant phenotypes of these genes account for some but not all ERK-regulated processes. To obtain molecular insight into how ERK signaling controls multiple biological processes in vivo through substrates, we devised an integrated bioinformatic, genetic, and biochemical approach by using *C. elegans* germ-line development as the model system.

In *C. elegans* RAS and ERK are encoded by *let-60* and *mpk-1*, respectively, and loss-of-function or null mutations in these core components abrogate pathway activity (1) (Fig. 1*A*). MPK-1 (ERK) controls fate specification during vulval development whereas during germ-line development, MPK-1 controls and coordinates at least seven distinct biological processes (11), ranging from developmental switches such as male germ cell fate specification to cell biological processes such as membrane organization and morphogenesis of pachytene cells (11) (Fig. 1*B*). Active MPK-1, as visualized by an antibody specific to the activated diphosphorylated form of the protein (dpMPK-1), displays a dynamic and stereotypical spatial localization pattern that correlates well with these characterized *mpk-1*-dependent processes in the germ line (11) (Fig. 1*B*). However, no substrate has been identified that controls any of these processes. Using a functional genomic approach we identify at least

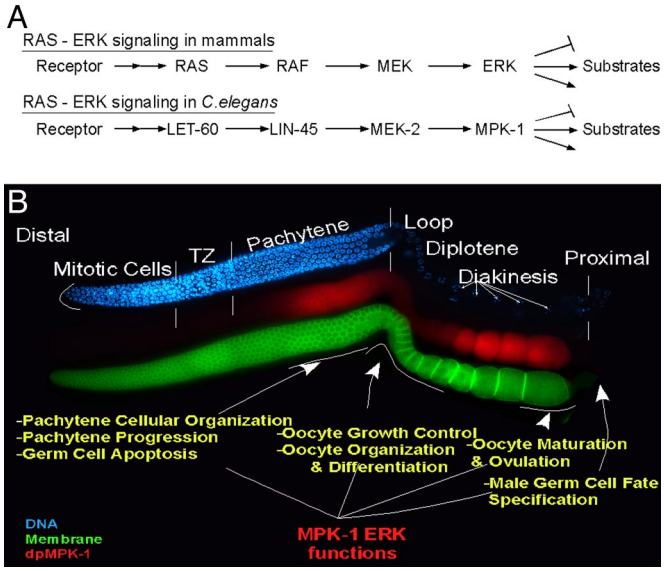

Fig. 1. MPK-1 signaling controls seven biological processes during *C. elegans* germ-line development. (*A*) Schematic of the conserved RAS–ERK signaling pathway in mammals and *C. elegans*. ERK/MPK-1 activates or inactivates substrate proteins via phosphorylation. (*B*) MPK-1 controls seven biological processes during germ-line development (11). Fluorescent micrograph of a dissected *C. elegans* adult hermaphrodite gonad showing chromosome (blue), activated dpMPK-1 (red), and membrane (green) morphology as germ cells progress through oogenesis. The seven MPK-1 controlled germ-line processes examined in this study are indicated (11) (Fig. S1).

Author contributions: S.A. and T.S. designed research; S.A., M.O., S.N., M.H., A.M., and A.H. performed research; A.G. contributed new reagents/analytic tools; S.A. and T.S. analyzed data; and S.A. and T.S. wrote the paper.

The authors declare no conflict of interest.

This article is a PNAS Direct Submission.

[1]Present address: Department of Biology, College of New Jersey, Ewing, NJ 08628-0718.

[2]To whom correspondence should be addressed at: 4566 Scott Avenue, Department of Genetics, Washington University School of Medicine, St. Louis, MO. E-mail: ts@genetics.wustl.edu.

This article contains supporting information online at www.pnas.org/cgi/content/full/0812285106/DCSupplemental.

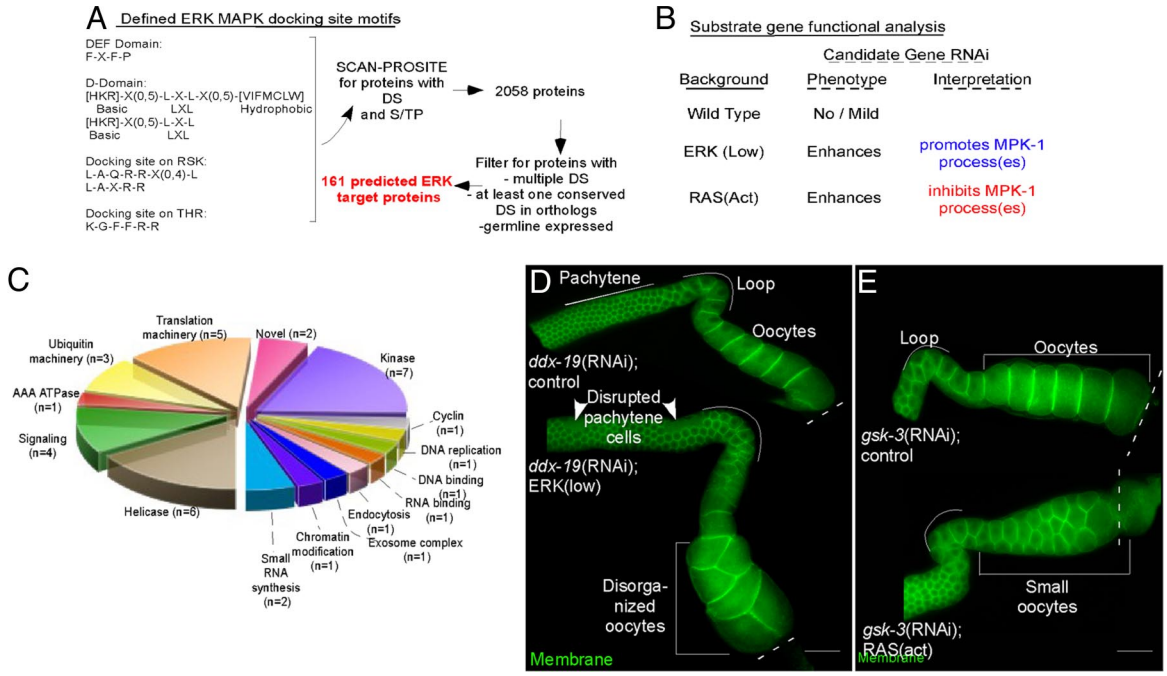

Fig. 2. *In silico* and genetic enhancer screen identifies 37 candidate MPK-1 substrates that function during germ-line development. (*A*) Outline of bioinformatics approach and sequences of characterized ERK-docking sites (DS). (*B*) Genetic logic used in the enhancer screen to identify genes that promote or inhibit MPK-1 pathway function. Wild-type control and sensitized backgrounds contain the *rrf-1(pk1417)* mutation, which prevents RNAi in the soma but not the germ line (29). At the permissive temperature where the RNAi screen was performed, *mpk-1(ga111ts)* ERK has lower MPK-1 activation whereas *let-60(ga89ts)* RAS has elevated/ectopic MPK-1 activation. (*C*) Pie chart showing predicted molecular functions of 37 genes that enhance one or the other sensitized genetic background (Dataset S2). (*D*) Fluorescent micrographs illustrating *ddx-19* RNAi enhancement of *rrf-1*; *mpk-1(ga111ts)*. (*E*) Fluorescent micrographs illustrating *gsk-3* attenuated RNAi enhancement of *rrf-1;let-60(ga89ts)*. (Scale bar, 20 μm.)

30 conserved ERK substrates that each executes distinct germ-line processes. Our results provide a global view of how ERK, a central regulator downstream to many receptor signaling pathways, yields distinct biological outcomes in a single tissue by controlling multiple diverse substrates.

Results and Discussion

Integrated Bioinformatic, Genetic, and Biochemical Analysis Identifies 30 in Vivo ERK Substrates. ERK recognizes substrates via specific amino acid signatures, called-docking sites (12). Docking sites provide high-affinity interaction between ERK and the substrate, allowing efficient phosphorylation of the substrate at appropriate phosphoacceptor sites (S/TP) (13). Based on the premise that unidentified MPK-1 substrates contain ERK-docking and phosphoacceptor sites, we scanned the *C. elegans* proteome for proteins that harbor one or more of four characterized ERK-docking sites: D domain (14) and its variant (RSK domain, 15); the DEF domain (8); and the docking motif characterized in the thyroid hormone receptor (16) [Fig. 2*A* and supporting information (SI) *Methods*]. The scan recovered 2,058 proteins that carry at least one ERK-docking site and a potential phosphoacceptor site(s) within 100 aa. Given the low information content of the docking-site motifs, some proteins likely carry the motif simply by chance. To reduce false predictions and obtain a higher probability set before labor-intensive validation screens, four additional stringent filters were imposed (Fig. 2*B* and *SI Methods*). (*i*) The predicted docking and phosphoacceptor sites must reside in an intracellular domain of a protein. (*ii*) Each protein must contain two or more predicted ERK-docking sites. (*iii*) We used reciprocal best BLAST analysis and ClustalW alignments to demand that each protein have an ortholog in the human proteome, with at least one ERK-docking site conserved positionally between the orthologs; Dataset S1*b* lists these 258 proteins. (*iv*) Each protein must be expressed in the *C. elegans* germ line, based on analysis of two available microarray databases (17; C. Hunter, personal communication) and an RNA in situ hybridization database (*SI Methods*). Application of these criteria yielded 161 high-priority candidates, with multiple ERK-docking sites, at least one of which is conserved in humans (Dataset S1*a*). More than 95% of the 161 candidates have not been implicated to function downstream to ERK in any system, thus our analysis may have enriched for unknown ERK substrates.

To determine whether the 161 candidates function in vivo to govern any of the seven MPK-1-dependent biological process(es) in the *C. elegans* germ line, we conducted an RNAi-based genetic enhancer screen (Fig. 2*B*). The function of each gene was reduced specifically in the germ line of wild-type control worms and in the germ line of two sensitized genetic backgrounds that exhibit decreased or increased levels of active MPK-1 (11) (Fig. 2*B* and *SI Methods*). The effect of RNAi on each MPK-1-dependent germline process was assessed by immunofluorescence microscopy of dissected germ lines and differential interference contrast microscopy-based analysis of intact worms (Fig. S1 and Dataset S1).

mpk-1(ga111ts) is a temperature-sensitive (ts) loss-of-function allele (18) that at permissive temperature exhibits a wild-type phenotype despite decreased levels of active MPK-1 (11). Here, MPK-1 likely phosphorylates substrates at lower levels than wild type. Thus, we reasoned that if RNAi of a candidate gene produces an *mpk-1*-like loss-of-function phenotype, then its gene product normally functions to promote the given *mpk-1*-dependent event and phosphorylation likely activates its function. In contrast, *let-60(ga89ts)* is a ts gain-of-function mutant (19) that displays a wild-type phenotype at the permissive temperature despite elevated levels and ectopic active MPK-1 (11). Here, MPK-1 likely phosphorylates substrates at inappropriate spatial regions of the germ line. In this case, we reasoned that if RNAi of a candidate gene specifically produces a gain-of-function phenotype, then the encoded product normally functions to inhibit the given *mpk-1*-

GENETICS

dependent process, and phosphorylation likely inactivates its function (Fig. 2*B*).

Functional analysis by RNAi revealed that 37 (23%) of the 161 candidates regulate specific MPK-1-dependent biological processes during *C. elegans* germ-line development (Fig. 2*C* and Dataset S1*a*). Interestingly, we were able to identify a genetic interactor for each of the seven MPK-1-dependent germ-line events assayed (Fig. S1), and in all cases more than one gene product contributes to the execution of each biological process (Fig. 3*A* and Dataset S1*a*). RNAi of 26 genes enhance the MPK-1 loss-of-function background at permissive temperature and likely promote pathway function (Dataset S1*a*, shaded blue). For example, RNAi of the DEAD box helicase T07D4.4 (here named DDX-19) does not produce any germ-line phenotype in control or *let-60(ga89ts)* worms but in *mpk-1(ga111ts)* leads to disrupted membrane organization of pachytene cells and disorganized oocytes in 20% and 25% of germ lines, respectively (Fig. 2*D* and Dataset S2). Thus, *ddx-19* functions to promote normal membrane organization of pachytene cells and oocyte organization and differentiation (Fig. 3*A*). RNAi of 11 gene products enhance the *let-60* RAS gain-of-function background at permissive temperature and thus likely inhibit pathway function (Dataset S1*a*, shaded green). For example, attenuated RNAi (*SI Methods*) of *gsk-3* had no effect on germ-line development of control worms or *mpk-1(ga111ts)*, but produced small oocytes in *let-60(ga89ts)* background in 30% of germ lines (Fig. 2*E* and Dataset S2). Thus, we infer that *gsk-3* inhibits the RAS–ERK pathway function and regulates oocyte growth. Because RNAi can sometimes cause off-target effects (20), we validated our results on 12 genes for which putative null deletion alleles were available. We found that the null alleles phenocopied the RNAi-induced genetic interactions in relevant double mutant backgrounds for 10 genes. Null allele of one gene shows a subset of *mpk-1* like germ-line phenotypes as a single mutant (*cgh-1*), while analysis of one was precluded because of essential roles in earlier development (Dataset S1*a*, Dataset S2, Dataset S3, and Fig. S2).

To assess whether any of the 37 genetic interactors encodes direct substrates of active ERK2, we conducted in vitro kinase assays on His_6- or GST-tagged fusion proteins of each interactor by using active murine ERK2 (8, 21). Besides a gel-based assay for phosphorylation, we performed kinetic analysis measuring the K_m and V_{max} to assess efficiency and specificity of the kinase reaction, using the relative acceptor ratio (RAR = V_{max}/K_m) as an overall measure of the protein as a substrate (8, 22). ERK2-dependent phosphorylation of myelin basic protein (MBP) was set as baseline. MBP is frequently used as a substrate to assay ERK activity because it contains many phosphoacceptors; however, because it lacks known ERK-docking sites it can be used to assess high-affinity interactions between ERK2 kinase and its substrate. From the kinetic analysis, 30 (85%) candidates are robust in vitro ERK2 substrates, using the conservative requirement of an RAR >4 (Table S1). Consistent with phosphorylation by ERK2 occurring via a high-affinity interaction in all likelihood because of docking sites, 29 of 30 have a K_m of <1 μM. In summary, our genetic and biochemical tests identified 30 conserved ERK substrates, with each participating in at least one MPK-1-dependent biological process (Fig. 3*A*, Dataset S1, and Table S1).

Phosphorylation of DDX-19 and GSK-3 in Vivo Depends on MPK-1. To provide further support that the 30 proteins identified are in vivo MPK-1 substrates, we tested 2 for MPK-1-dependent phosphorylation in vivo by using phosphospecific antibodies. DDX-19 is a robust in vitro substrate of active ERK2 and carries 2 conserved putative ERK phosphoacceptor sites S612 and T745 (Fig. 4*A* and Table S1). To map the ERK-dependent sites of phosphorylation, when one or the other of these residues was replaced with alanine, phosphorylation of DDX-19 was reduced (decreased V_{max}, unchanged K_m) (Fig. 4*B*); it was eliminated when both residues were altered, indicating that S612 and T745 are major in vitro ERK2

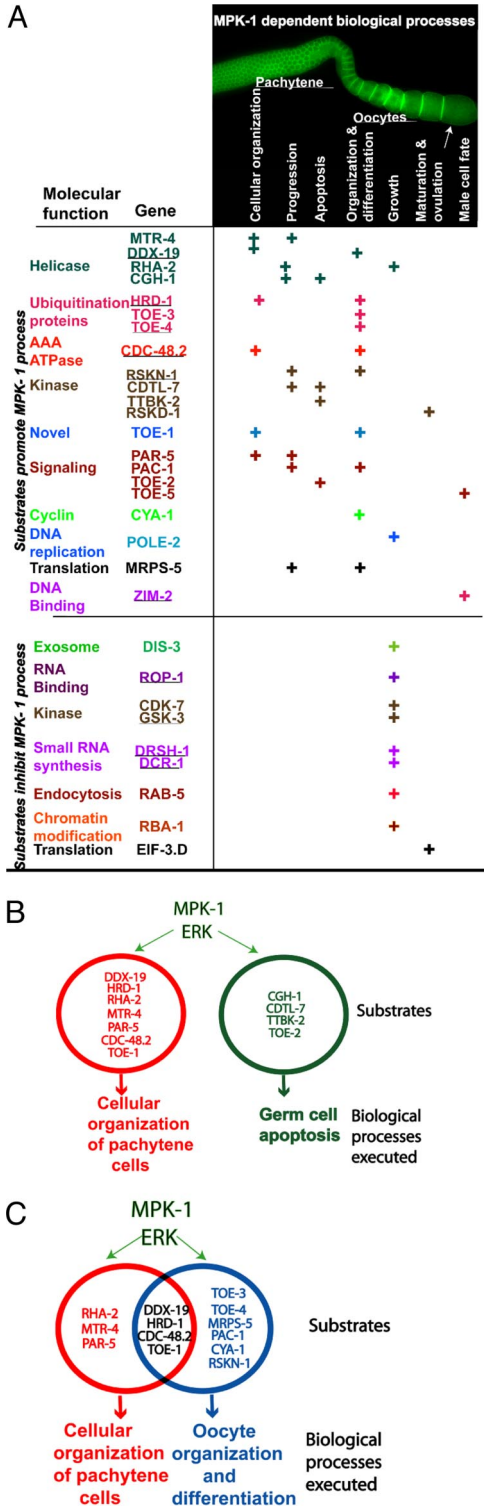

Fig. 3. Multiple molecularly diverse substrates function in each MPK-1-dependent process. (*A*) (*Top*) Seven MPK-1-dependent processes, shown relative to adult hermaphrodite germ-line development. (*Middle* and *Bottom*) Thirty in vitro ERK2 substrates and their functional molecular categories. +, Germ-line process in which a given substrate functions. Analysis with null alleles for 10 substrates (underlined) (Dataset S2), reveals concordant results with RNAi screen. For oocyte growth control, two substrates enhance *mpk-1(ga111ts)* and produce large oocytes whereas eight enhance *let-60(ga89ts)* and produce small oocytes (Fig. S1). (*B*) Nonoverlapping groups of MPK-1 substrates execute pachytene cellular organization (red circle, 7 genes) and germ cell apoptosis (green circle, 4 genes). (*C*) Partially overlapping groups of substrates regulate pachytene cellular organization (red) and/or oocyte organization and differentiation (blue).

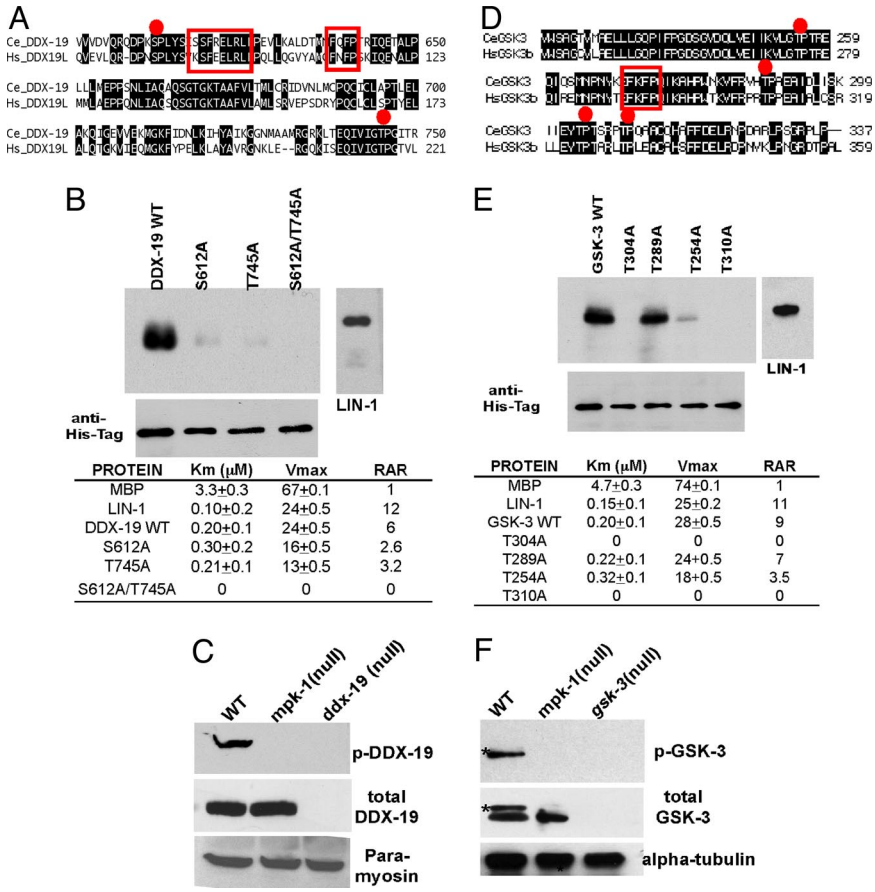

PROTEIN	Km (μM)	Vmax	RAR
MBP	3.3±0.3	67±0.1	1
LIN-1	0.10±0.2	24±0.5	12
DDX-19 WT	0.20±0.1	24±0.5	6
S612A	0.30±0.2	16±0.5	2.6
T745A	0.21±0.1	13±0.5	3.2
S612A/T745A	0	0	0

PROTEIN	Km (μM)	Vmax	RAR
MBP	4.7±0.3	74±0.1	1
LIN-1	0.15±0.1	25±0.2	11
GSK-3 WT	0.20±0.1	28±0.5	9
T304A	0	0	0
T289A	0.22±0.1	24+0.5	7
T254A	0.32±0.1	18+0.5	3.5
T310A	0	0	0

Fig. 4. DDX-19 and GSK-3 phosphorylation is MPK-1-dependent in vivo. (*A* and *D*) ClustalW protein alignment of *C. elegans* and human orthologs of DDX-19 (*A*) identifies two conserved phosphoacceptors (S612 and T745; red circles) and two conserved docking sites (red boxes) and GSK-3 (*D*) identifies four conserved phosphoacceptor sites (T254, T289, T304, and T310; red circles) and two conserved docking sites (one shown here, red boxes) (Fig. S4). Mapping of ERK2 phosphoacceptors for (*B*) DDX-19 and (*E*) GSK-3 using in vitro kinase assays and site-directed mutagenesis (*SI Methods*). (*B* and *D*) (*Top*) ^{32}P incorporation into indicated proteins. (*Middle*) Western blot analysis by using anti-HIS antibody for loading control. (*Bottom*) Kinetic analyses were performed on wild-type and all phosphoacceptor mutant proteins (S/T to A). Values for K_m and V_{max} (average ± 1 SD of five experiments) were used to calculate the RAR, which was normalized to 1, relative to MBP. LIN-1 is a positive control. (*C* and *F*) Western blot analysis of protein extracts from wild-type (WT), *mpk-1(ga117)*-null, and (*C*) *ddx-19(ok783)*-null or (*F*) *gsk-3(nr2047)*-null animals probed with antibodies specific for (*C*) phospho-DDX-19 (pS612 and pT745), total DDX-19, and paramyosin (loading control), (*F*) phospho-GSK-3 (pT304 and pT310), total GSK-3, and α-tubulin (loading control). The antibodies are specific to the gene product tested because no species was detected in the respective null mutant. DDX-19 is phosphorylated on S612 and/or T745 in WT but not *mpk-1* null. *, slower-mobility GSK-3 band detected with total GSK-3 antibody that comigrates with the species detected with the phospho-GSK-3 antibody. In *mpk-1*-null, this band is not detected on short exposures; however, on longer exposures, a weak band is visible (also weakly detected by total-GSK-3 antibody).

phosphorylation sites in this protein (Fig. 4*B* and Fig. S2). Next, we generated antibodies specific to the phosphorylated form of DDX-19 at S612 and T745 and conducted Western blot analysis on wild-type, *ddx-19*-null and *mpk-1*-null mutant animals (Fig. S3). Our analysis revealed that DDX-19 is phosphorylated in vivo in an *mpk-1*-dependent manner (Fig. 4*C*). Taken together, our work on DDX-19 suggests that MPK-1 phosphorylates DDX-19 on S612 and/or T745 in vivo to promote pachytene cellular organization and oocyte organization and differentiation.

Glycogen synthase kinase 3 (GSK-3) carries four conserved phosphoacceptors in worms T254, T295, T304, and T310 (Fig. 4*D*). Ding et al. (23) reported that active ERK2 phosphorylates human GSK-3β at residue T43; however, the corresponding +1 proline (P44) of human GSK-3β is not present in *C. elegans* GSK-3, making it an unlikely ERK phosphoacceptor (Fig. S4). To map the ERK-dependent phosphorylation, we singly replaced each of the four conserved phosphoacceptor residues in GSK-3 with alanine and tested the resulting proteins as substrates of ERK2 in vitro (Fig. 4*E*). Residues T304 and T310 appear to be major phosphoacceptor sites because each mutant abolished phosphorylation by ERK2 in vitro. As with DDX-19, the generation of antibodies specific for the phosphorylated forms of these epitopes (T304/T310; see *SI Methods*) together with Western blot analysis on wild-type, *gsk-3*-null, and *mpk-1*-null worms revealed that GSK-3 is phosphorylated at T304 and/or T310 in vivo, in an *mpk-1*-dependent manner (Fig. 4*F*). Our finding that both DDX-19 and GSK-3 are phosphorylated in vivo in an MPK-1-dependent manner suggests that MPK-1 acts directly through most, if not all, of the remaining 28 identified substrates to control germ-line development.

Conserved Substrates May Function Downstream of ERK in Mammals. The human orthologs of the 30 MPK-1 substrates identified here contain conserved ERK-docking sites and phosphoacceptor sites (Dataset S1*a* and Table S1). To address whether some of these orthologs act as ERK substrates in humans, we conducted in vitro ERK2 kinase assays on two human proteins 14-3-3 ζ and p97, orthologs of worm PAR-5 and CDC-48.2. We found that both proteins are phosphorylated by ERK2 on the same conserved phosphoacceptor sites as used in the worm proteins (Fig. S5), suggesting that many of these orthologs serve as ERK substrates in humans. In support of this, prior work identified GSK-3β (23) and RSK-4 (ortholog of RSKN-1) (24) as ERK substrates in mammals.

GENETICS

The human orthologs of another five of the MPK-1 substrates we identified (PAC-1, POLE-2, DIS-3, CDK-7, and RBA-1) were found to be phosphorylated in mass spectrometry studies of EGF-stimulated HeLa cells (7). Our results add to the proteomic study by providing independent evidence that ERK is the protein kinase likely responsible for phosphorylation of these proteins and by extension suggest that they function in ERK-regulated developmental events.

Multiple Molecularly Diverse ERK Substrates Govern Individual Biological Processes. Active MPK-1 controls seven different biological processes during germ-line development, ranging from cell-biological processes to cell fate decisions (Fig. 1*B*). We find that MPK-1 controls biological processes through substrates belonging to at least 15 functional classes of proteins, including RNA helicases and kinases, and proteins functioning in many aspects of cellular machinery such as ubiquitination, biogenesis of small RNAs, chromatin modification, and DNA replication. Interestingly, we could not assign any one class of proteins to a specific biological process (Fig. 3*A*). Instead, we find that MPK-1 coordinately regulates multiple functionally distinct substrates to execute each individual biological process. For example, MPK-1 acts through RNA helicases (MTR-4, DDX-19, RHA-2), a ubiquitin ligase (HRD-1), an AAA ATPase (CDC-48.2), a conserved protein (TOE-1), and an adaptor protein (PAR-5) to govern pachytene cellular organization (Fig. 3*A*). Identification of many gene products governing one process suggests that active MPK-1 coordinates the function of multiple substrates, through phosphorylation, to execute an individual process. Additionally, the utilization of multiple substrates by MPK-1, to govern a single biological process, seems to provide robustness to MPK-1 pathway outcome, wherein loss of any one substrate may not result in a severe MPK-1-like mutant phenotype. We found that for some substrates, null mutations either had no obvious MPK-1 pathway defects (e.g., *ddx-19*, *rop-1*) or had mild MPK-1 pathway defects (e.g., *cgh-1*) (Dataset S2). In either case, the MPK-1-dependent processes were further compromised in a sensitized genetic background (e.g., *ddx-19*) (Fig. S2*C* and Dataset S2). A model that emerges is that at least some of the molecularly diverse MPK-1 substrates likely function redundantly to execute each individual biological process. Multiplicity of ERK substrates in governing individual biological processes may also hold true in other systems. For instance, two substrates MISS (25) and DOC1R (26) participate in ERK-dependent control of spindle integrity during MII arrest in mouse oocytes. Together, our data suggest that contemporaneous phosphorylation of diverse substrates by active ERK modulates different aspects of cellular machinery, eventually converging to execute an individual process.

How Might ERK Signaling Through Substrates Yield Unique Biological Outcomes? A key question in developmental signaling is how one pathway executes a wide variety of biological processes. Our data indicate that MPK-1 acts through different combinations of substrates to produce distinct biological outcomes (Fig. 3*A*). Although this inference is based on RNAi of 30 substrates, which may underestimate function because of partial knockdown, it is fully supported by analysis of null alleles for 11 substrate genes (Dataset S2). For example, we find that MPK-1 executes the distinct yet spatially overlapping biological processes of pachytene cellular organization and germ cell apoptosis by acting through two different combinations of substrates. MPK-1 governs the organization of pachytene cells by phosphorylation of seven substrates: DDX-19, HRD-1, RHA-2, MTR-4, PAR-5, CDC-48.2, and TOE-1 (Fig. 3*B*). Whereas in the same pachytene germ cells, MPK-1 governs germ cell apoptosis by acting through a mutually exclusive set of four substrates: CGH-1, CDTL-7, TTBK-2, and TOE-2 (Fig. 3*B* and Fig. S1). Thus, MPK-1 appears to regulate these two distinct processes simultaneously in the same cells by acting through nonoverlapping sets of substrates, at least for substrates thus far identified.

A

MPK-1 substrates function to reinforce or attenuate active MPK-1 signal

Gene	Effect of RNAi on dpMPK-1	Feedback prediction	Function
par-5	lower in pachytene	Positive regulator	Promotes MPK-1 signaling
pole-2	lower in pachytene and diplotene oocytes	Positive regulator	Promotes MPK-1 signaling
rba-1	higher in diplotene oocytes	Negative regulator	Inhibits MPK-1 signaling
gsk-3	higher in diplotene oocytes	Negative regulator	Inhibits MPK-1 signaling
cdk-7	higher in diplotene oocytes	Negative regulator	Inhibits MPK-1 signaling
dcr-1	higher in diplotene oocytes	Negative regulator	Inhibits MPK-1 signaling
drsh-1	higher in diplotene oocytes	Negative regulator	Inhibits MPK-1 signaling
rab-5	higher in diplotene oocytes	Negative regulator	Inhibits MPK-1 signaling
rskn-1	higher in diplotene oocytes	Negative regulator	Promotes MPK-1 signaling
cya-1	higher in diplotene oocytes	Negative regulator	Promotes MPK-1 signaling

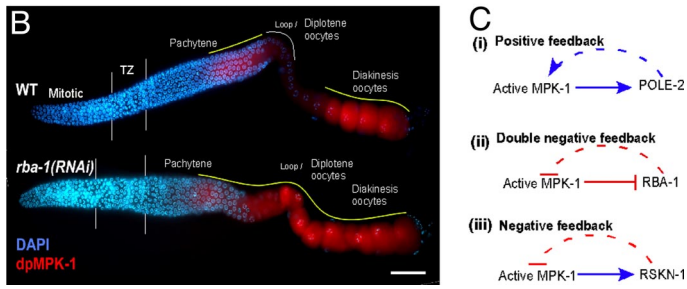

Fig. 5. MPK-1 substrates function to regulate MPK-1 activation in feedback loops. (*A*) Ten MPK-1 substrates regulate MPK-1 activation and fall into three categories. (*B*) Fluorescent micrographs of dissected *rrf-1* null gonads, after either *gfp* RNAi (*Upper*) or *rba-1* RNAi (*Lower*), stained for dpMPK-1 (red) or DNA (blue). (Scale bar, 20 μm.) (*C*) Models of possible regulatory feedback loops through which substrates modulate germ-line MPK-1 activation.

For some MPK-1-dependent processes, we observe a significant overlap between substrates as shown for processes pachytene cellular organization and oocyte organization and differentiation (Fig. 3*C*, black). However, despite this overlap there are at least three nonoverlapping substrates that help execute pachytene cellular organization and six for oocyte organization and differentiation (Fig. 3*C*). These findings suggest that MPK-1-dependent phosphorylation of substrates in different combinations may bring together diverse cellular pathways in unique assortments to result in distinct biological outcomes.

Feedback Regulation, by Substrates, Can Reinforce or Attenuate ERK Activation. Analysis of MPK-1 substrates revealed that 10 of the 30 impinge on the spatial pattern of active MPK-1 (Fig. 5*A*). Activated MPK-1 displays a stereotypical pattern with a region of up-regulation in proximal pachytene, followed by down-regulation in the loop/diplotene, followed by up-regulation in the diakinesis oocytes (Fig. 1*B*). This dynamic spatially restricted activation pattern of MPK-1 is critical for normal germ-line development because perturbations to it can result in mutant phenotypes (11, 27). We observed that RNAi of 10 substrate genes in control germ lines altered the activation pattern of MPK-1, as visualized by staining with dpMPK-1 antibody (Fig. 5 *A* and *B*). These substrates can be divided into two major types based on their regulation of dpMPK-1 accumulation. The first type comprises substrates that reinforce MPK-1 signal strength and function as positive regulators of MPK-1 activation (Fig. 5*A*, blue). RNAi of *par-5* and *pole-2* in the control background leads to lower accumulation of dpMPK-1 in pachytene and both pachytene and oocytes, respectively (Fig. 5*A*, blue). Our genetic studies reveal that PAR-5 and POLE-2 promote the MPK-1-dependent biological processes of pachytene progression and cellular organization, and oocyte growth, respectively (Fig. 3*A*,

Dataset S1, and Fig. S1). Thus, PAR-5 and POLE-2 may regulate these *mpk*-1-dependent processes simply as a consequence of promoting MPK-1 activation, possibly as part of a positive feedback loop (Fig. 5*Ci*).

The second type is composed of substrates that attenuate MPK-1 signal strength and function as negative regulators of active MPK-1 (Fig. 5*A*). RNAi of eight genes (e.g., *rba-1*) (Fig. 5*B*, green) causes an increase in dpMPK-1 in the loop/diplotene region in the control background. Of these, RNAi of six (Fig. 5*A*, light green) also enhances *let-60* RAS gain-of-function, indicative of a function to inhibit MPK-1-dependent processes (Figs. 2*B* and 3*A* and Dataset S1). Accumulation of active MPK-1, on RNAi of these six genes, may increase MPK-1 signaling in a *let-60* RAS gain-of-function mutant background to a point above the threshold at which gain-of-function phenotype is visible. Thus, these six substrates may affect MPK-1-dependent processes simply by attenuating levels of activated MPK-1, possibly as part of a double-negative feedback loop (Fig. 5*Cii*).

In contrast, two of the eight (RSKN-1 and CYA-1, dark green) negative regulators, do not affect the *let-60* RAS gain-of-function background; instead, these function to promote MPK-1 signaling and affect the *mpk-1* loss-of-function background (Fig. 3*A* and Dataset S2). These substrates thus appear to have two functions: one to attenuate ERK signal strength (Fig. 5 *A* and 5*Ciii*) and the other to promote distinct MPK-1-dependent biological outcomes, pachytene progression (RSKN-1) (Fig. 3*A*), and oocyte organization and differentiation (RSKN-1, CYA-1) (Fig. 3*A*). Prior work suggests that the mouse ortholog of RSKN-1, RSK4, is also a negative regulator of active ERK signal (28), making it likely that at least some of the other nine MPK-1 substrates also function in feedback regulation of ERK in other organisms. Because none of these genes is a dual-specificity phosphatase, future work aimed at elucidating how these regulatory loops help establish and maintain the spatially restricted patterns of MPK-1 activity in the germ line will unravel the molecular basis of this regulation. Taken together, our observations that 10 of the 30 MPK-1 substrates govern MPK-1 activity levels via feedback regulation underlines the importance of such mechanisms in modulating the strength, duration, and spatial limits of MPK-1 activity during development.

Methods

In Silico Analysis. Initial scan on *C. elegans* proteome at SCAN PROSITE conducted on Wormpep version WS109 for proteins with ERK-docking sites yielded 2,058 proteins (*SI Methods* and Table S1). Transmembrane predictions were identified with TMHMM-2.0 and TMPRED programs (*SI Methods*). Human orthologs were identified by reciprocal best BLAST analysis at National Center for Biotechnology Information (*SI Methods*). Conservation of docking sites was determined by manual inspection of alignments between the worm and the human sequences (Fig. 2 *A* and *D* and Fig. S4) in Megalign by using ClustalW. Protein domains were identified by a combination of PFAM and Conserved Domain Architecture Retrieval tool (*SI Methods*); 258 proteins had at least one conserved docking site (Dataset S1*b*). Of these, 161 showed germ-line expression per available worm in situ hybridization database at NEXTDB and microarray data (*SI Methods*) (17; C. Hunter, personal communication). Details are provided in *SI Methods*.

RNAi Genetic Enhancer Screen. F1 feeding RNAi was performed as described (*SI Methods*) (11) in the control and the two sensitized backgrounds at the permissive temperature (20 °C). All positives were retested at least three times (*SI Methods*). This analysis yielded 18 of 161 candidate genes that specifically enhanced either sensitized genetic background. Seventy genes did not show phenotypes in any background.

RNAi of 73 genes produced strong phenotypes in the control *rrf-1* background, distinct from characterized *mpk-1* phenotypes (Dataset S1) (11). Here, RNAi knockdown was attenuated by limiting the exposure of worms to dsRNA until no phenotype was observed in the control background and then retested in the two sensitized backgrounds. Attenuation was performed by either (*i*) placing embryos on RNAi plates followed by analysis of adults at 24 h past L4 developmental stage or (*ii*) placing L4 worms that received RNAi only for 24 h (*SI Methods*). This was the P0 analysis.

ACKNOWLEDGMENTS. We thank Drs. K. Kornfeld, M. Sundaram, J. Skeath, A. Kalia, D. Hansen, M. Dorsett, S. Dutcher, and M. Johnston for insightful comments on the manuscript. We are grateful to our colleagues for reagents, Dr. Andrey Shaw (14-3-3-GST) and Dr. Phyllis Hanson (p97) (Washington University School of Medicine, St. Louis). M.H. and A.H. were supported by the Howard Hughes Medical Institute Undergraduate Education Research Program, and A.M. was supported by the Siteman Cancer Center summer student program. Work in the T.S. laboratory was supported by National Science Foundation Grant 0416502 and National Institutes of Health Grant GM63310. A.G. was supported by the Intramural Research Program at the National Institute of Diabetes and Digestive and Kidney Diseases/National Institutes of Health.

1. Moghal N, Sternberg PW (2003) The epidermal growth factor system in *Caenorhabditis elegans*. *Exp Cell Res* 284:150–159.
2. Chen Z, et al. (2001) MAP kinases. *Chem Rev* 101:2449–2476.
3. Ku H, Meier KE (2000) Phosphorylation of paxillin via the ERK mitogen-activated protein kinase cascade in EL4 thymoma cells. *J Biol Chem* 275:11333–11340.
4. Gille H, et al. (1995) ERK phosphorylation potentiates Elk-1-mediated ternary complex formation and transactivation. *EMBO J* 14:951–962.
5. Roux PP, Ballif BA, Anjum R, Gygi SP, Blenis J (2004) Tumor-promoting phorbol esters and activated Ras inactivate the tuberous sclerosis tumor suppressor complex via p90 ribosomal S6 kinase. *Proc Natl Acad Sci USA* 101:13489–13494.
6. Lewis TS, et al. (2000) Identification of novel MAP kinase pathway signaling targets by functional proteomics and mass spectrometry. *Mol Cell* 6:1343–1354.
7. Olsen JV, et al. (2006) Global, in vivo, and site-specific phosphorylation dynamics in signaling networks. *Cell* 127:635–648.
8. Jacobs D, Beitel GJ, Clark SG, Horvitz HR, Kornfeld K (1998) Gain-of-function mutations in the *Caenorhabditis elegans* lin-1 ETS gene identify a C-terminal regulatory domain phosphorylated by ERK MAP kinase. *Genetics* 149:1809–1822.
9. Tan PB, Lackner MR, Kim SK (1998) MAP kinase signaling specificity mediated by the LIN-1 Ets/LIN-31 WH transcription factor complex during *C. elegans* vulval induction. *Cell* 93:569–580.
10. Brunner D, et al. (1994) The ETS domain protein pointed-P2 is a target of MAP kinase in the sevenless signal transduction pathway. *Nature* 370:386–389.
11. Lee MH, et al. (2007) Multiple functions and dynamic activation of MPK-1 extracellular signal-regulated kinase signaling in *Caenorhabditis elegans* germ-line development. *Genetics* 177:2039–2062.
12. Sharrocks AD, Yang SH, Galanis A (2000) Docking domains and substrate-specificity determination for MAP kinases. *Trends Biochem Sci* 25:448–453.
13. Karin M, et al. (1995) The regulation of AP-1 activity by mitogen-activated protein kinases. *J Biol Chem* 270:16483–16486.
14. Hibi A, Lin A, Smeal T, Minden A, Karin M (1993) Identification of an oncoprotein and a UV-responsive kinase that binds to and potentiates the cJUN activation domain. *Genes Dev* 7:2135–2148.
15. Smith JA, Poteet-Smith CE, Malarkey K, Sturgill TW (1999) Identification of an extracellular signal-regulated kinase (ERK)-docking site in ribosomal S6 kinase, a sequence critical for activation by ERK in vivo. *J Biol Chem* 274:2893–2898.
16. Lin HY, et al. (2003) Identification of the putative MAP kinase docking site in the thyroid hormone receptor-β1 DNA-binding domain: Functional consequences of mutations at the docking site. *Biochemistry* 42:7571–7579.
17. Reinke V, et al. (2000) A global profile of germ-line gene expression in *C. elegans*. *Mol Cell* 6:605–616.
18. Lackner MR, Kim SK (1998) Genetic analysis of the *Caenorhabditis elegans* MAP kinase gene *mpk-1*. *Genetics* 150:103–117.
19. Eisenmann DM, Kim SK (1997) Mechanism of activation of the *Caenorhabditis elegans* ras homologue *let-60* by a novel, temperature-sensitive, gain-of-function mutation. *Genetics* 146:553–565.
20. Kulkarni MM, et al. (2006) Evidence of off-target effects associated with long dsRNAs in *Drosophila melanogaster* cell-based assays. *Nat Methods* 3:833–838.
21. Jacobs D, Glossip D, Xing H, Muslin AJ, Kornfeld K (1999) Multiple docking sites on substrate proteins form a modular system that mediates recognition by ERK MAP kinase. *Genes Dev* 13:163–175.
22. Alessi DR, Smythe C, Keyse SM (1993) The human CL100 gene encodes a Tyr/Thr-protein phosphatase which potently and specifically inactivates MAP kinase and suppresses its activation by oncogenic ras in *Xenopus* oocyte extracts. *Oncogene* 8:2015–2020.
23. Ding Q, et al. (2005) Erk associates with and primes GSK-3β for its inactivation resulting in up-regulation of β-catenin. *Mol Cell* 19:159–170.
24. Barrett CB, Erikson E, Maller JL (1992) A purified S6 kinase kinase from *Xenopus* eggs activates S6 kinase II and autophosphorylates on serine, threonine, and tyrosine residues. *J Biol Chem* 267:4408–4415.
25. Lefebvre C, et al. (2002) Meiotic spindle stability depends on MAPK-interacting and spindle-stabilizing protein (MISS), a new MAPK substrate. *J Cell Biol* 157:603–613.
26. Terret ME, et al. (2003) DOC1R: A MAP kinase substrate that control microtubule organization of metaphase II mouse oocytes. *Development* 130:5169–5177.
27. Govindan JA, Cheng H, Harris JE, Greenstein D (2006) Gαo/i and Gαs signaling function in parallel with the MSP/Eph receptor to control meiotic diapause in *C. elegans*. *Curr Biol* 16:1257–1268.
28. Myers AP, Corson LB, Rossant J, Baker JC (2004) Characterization of mouse Rsk4 as an inhibitor of fibroblast growth factor–RAS–extracellular signal-regulated kinase signaling. *Mol Cell Biol* 24:4255–4266.
29. Sijen T, et al. (2001) On the role of RNA amplification in dsRNA-triggered gene silencing. *Cell* 107:465–476.

GENETICS